PHYSICAL REVIEW A VOLUME 17, NUMBER 6 JUNE 1978

Angular distribution of electrons elastically scattered from CO_2

T. W. Shyn, W. E. Sharp, and G. R. Carignan
Space Physics Research Laboratory, Department of Atmospheric and Oceanic Science, The University of Michigan, Ann Arbor, Michigan 48109
(Received 5 December 1977)

The angular distribution of electrons elastically scattered from CO_2 has been measured utilizing a crossed-beam method. The energy and angular ranges are 3.0 to 90.0 eV and −105° to +156°, respectively. The total elastic cross section and momentum-transfer cross sections have been determined. The total elastic cross section of CO_2 at 10.0 eV has been calibrated with respect to that of He at 10.0 eV, and the CO_2 cross section has been placed on an absolute scale by using the theoretical value of LaBahn and Calloway for He at 10.0 eV. The results are compared with theory and other experimental results with generally good agreement but with some noteworthy differences.

I. INTRODUCTION

Electron scattering from CO_2 in the broad energy range of 0.01–100 eV has been studied by several authors. Brüche[1] measured the total scattering cross sections in the energy range from 1 to 50 eV. Ramsauer and Kollath[2] have measured the angular distributions of the total cross sections in the energy range from 1.5 to 9.3 eV. Mohr and Nicoll[3] have measured the angular distributions of elastically and inelastically scattered electrons at the incident energy of 84 eV. Recently, a considerable amount of investigation on the vibrational-excitation cross sections has been done. Lassettre[4] has studied the incident energies of 48 and 58 eV and Geiger and Wittmaack[5] have measured vibrational excitations by 25-keV electrons. Also Schulz and collaborators[6] and Andrick *et al.*[7] have studied the vibrational-excitation cross section and the total inelastic cross section near the 3.8-eV resonance and at lower energies. The momentum-transfer cross section in the energy range 0.01–100 eV has been derived from swarm experiments by Phelps and collaborators.[8] More recently, Morrison *et al.*[9] have calculated, by means of a coupled-channels theory, total and differential electron scattering cross sections and the momentum-transfer cross section of CO_2 in the energy range 0.07–10 eV.

There are no extensive measurements of the angular distribution of electron-impact cross sections from CO_2 even for elastic scattering. The electron-impact scattering cross sections of CO_2 are important parameters for a number of reasons including understanding the atmospheres of Mars and Venus[10] whose major constituent is CO_2 and the study of the laser-fusion effect.[11]

This paper presents the results of an experiment in which the angular distributions of the elastically scattered electrons from CO_2 have been measured using a crossed-beam method. This work is an extension of the previous work on N_2.[12] The angular distribution for the differential cross sections by elastic scattering has been determined with monoenergetic electrons of energies from 3.0 to 90.0 eV, and for the angles −105° to +156°. The present measurements have been calibrated among themselves and have been placed on an absolute scale using the ratio of the cross sections of He and CO_2 and the theoretical value of LaBahn and Callaway[13] for helium at 10.0 eV.

II. APPARATUS AND PROCEDURE

The apparatus used for the electron scattering measurements is basically the same as that used previously for similar measurements of electron scattering from N_2 and has been described in the literature.[12] Two noteworthy improvements have been made: (i) The Vac-Ion pump has been replaced with a turbomolecular pump of greater speed and (ii) an additional set of Helmholtz coils has been added to the two existing coils to further reduce the residual field in the interaction region. The apparatus is shown in Fig. 1. A rotatable electron-beam source of 0.06 eV energy half-width interacts at 90° with a neutral beam collimated by a fused capillary array (Bendix product). Electrons scattered from the neutral beam are detected in a channeltron electron multiplier after passing through a 127° electrostatic energy analyzer.

The vacuum enclosure in which the measurements are taken is pumped by a 1500 l/sec turbomolecular pump backed by a mechanical forepump. Additionally a liquid-nitrogen-cooled cold plate is used and a background pressure of 10^{-9} torr is achieved. With the neutral beam on, the system pressure rises to about 10^{-6} torr and the density in the interaction region is more than 50 times greater than the overall system background density.

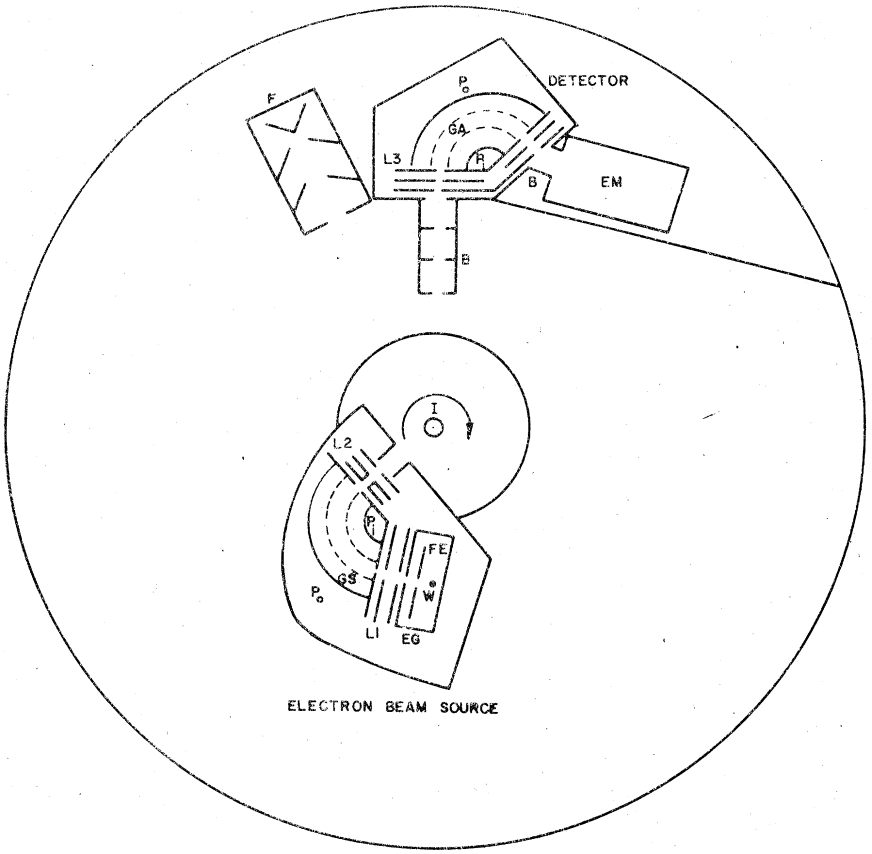

FIG. 1. Schematic diagram of appartus: W, filament; P_i, inner plate; EG, electron gun; I, interaction region; FE, focus electrode; B, baffle; L1, lens 1; L2, lens 2; L3, lens 3; L4, lens 4; P_o, outer plate; EM, electron multiplier; GS, grids of selector; GA, grids of analyzer; F, Faraday cup.

The magnetic field in the plane of measurement is reduced to less than 20 mG in all axes by compensation with the three Helmholtz coils. The measurement region is carefully shielded from all exposed potentials. The results at very low electron energies indicate that the measurement region is indeed field free.

The procedure for obtaining the measurements is as follows: The vacuum enclosure is pumped to its base pressure of 10^{-9} torr and the collimated beam of CO_2 is turned on and the signal count versus electron-beam angle is measured, integrating for 10 sec, each 6° from −105° to 156° at the selected beam energy. The measurement is repeated with the gas off to obtain the background count. The difference between the two signals is the angular distribution of elastically scattered electrons from the beam in the interaction region. To correct for the small-volume effect, a system pressure equal to that during the measurement is established through the capillary displaced from the interaction region and the angular dependence of the volume-scattered component is measured (a volume experiment). At 90° this contribution is 2% of the crossed-beam component. The true-zero

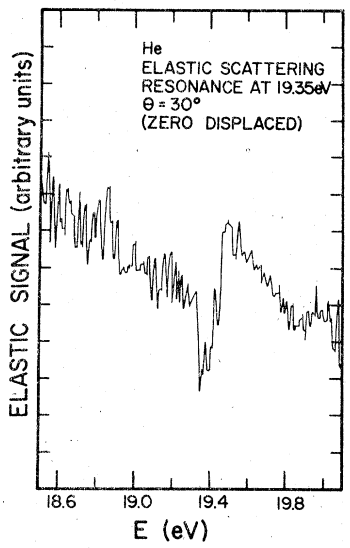

FIG. 2. Elastic scattering resonance in He in 19.35 eV and at 30°.

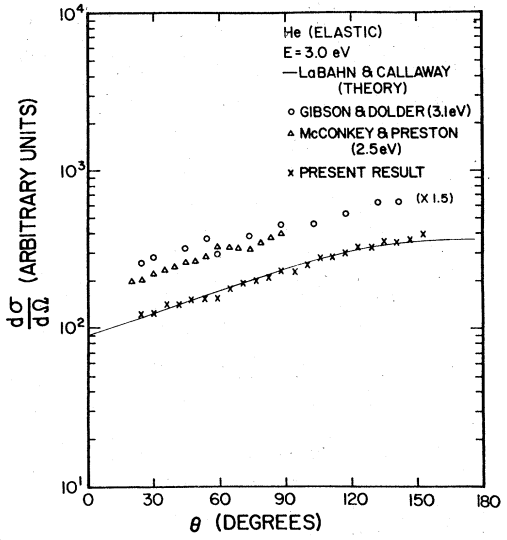

FIG. 3. Angular distribution per unit solid angle $d\sigma/d\Omega$ of He at 3.0 eV. Comparison of the measurements of Gibson and Dolder (Ref. 14), McConkey and Preston (Ref. 15) and theoretical value of LaBahn and Callaway (Ref. 13) with the present result. Data points of Gibson and Dolder (Ref. 14), and McConkey and Preston (Ref. 15) are raised 1.5 times for comparison.

scattering angle was determined from the symmetry of the angular distribution.

The apparatus is calibrated frequently during the measurement sequence. The absolute energy scale is established within ±0.05 eV using the helium-resonance feature at 19.35 eV as shown in Fig. 2. Also, for certain CO_2 data sets, an identical run is made using helium which enables a direct comparison to other experimental results. The measured ratio of the total elastic scattering cross sections at 10.0 eV is also used to established the absolute value of CO_2 cross section using the theoretical value of the total elastic cross section for helium of LaBahn and Callaway.[13] Figure 3 shows a typical angular distribution of elastically scattered electrons from He at 3.0 eV along with the theoretical results of LaBahn and Callaway[13] and the experimental results of Gibson and Dolder,[14] and McConkey and Preston.[15] The interpretation of the results obtained from this procedure is discussed in Sec. III.

III. EXPERIMENTAL RESULTS

Angular distribution data have been obtained at each of 14 impact energies (3.0, 3.5, 3.8, 4.0, 5.0, 7.0, 10.0, 15.0, 20.0, 30.0, 40.0, 50.0, 70.0, and 90.0 eV). To place each energy on the same relative cross-section scale, relative calibrations were run for each energy at 60° where the scattered intensities are relatively insensitive to angle. Five runs at each energy are taken and averaged and normalized to each order through the calibration at 60° using 10.0 eV as the reference; the results are tabulated in Table I. Additionally, the total elastic cross section of CO_2 at 10.0 eV was calibrated with respect to that of helium at 10.0 eV in a volume experiment (a static-gas target). Ten sets of calibration are run and averaged. This enables a derivation of the absolute cross section based on the theoretical value for helium at 10.0 eV calculated by LaBahn and Callaway.[13]

Figures 4–9 show the normalized angular distribution $d\sigma/d\Omega$ for nine incident energies.

The theoretical values of Morrison *et al.*,[9] at 4.0 eV and the experimental data of Mohr and Nicoll[3] at 84 eV are also shown in Figs. 5 and 9, respectively.

The maximum statistical uncertainty in any data point in these figures is ± 3%. The inter-energy calibration was repeatable to less than 10% in five different runs and the CO_2-He inter-calibration at 10.0 eV, although repeatable to less than 5%, could be subject to systematic errors estimated to be less than 10%.

At the low energies, the composite data in Fig. 4 show the transition from near-isotropic scattering at 3.0 eV to peaked forward scattering and backscattering at 5.0 eV. Near 3.8 eV (compound

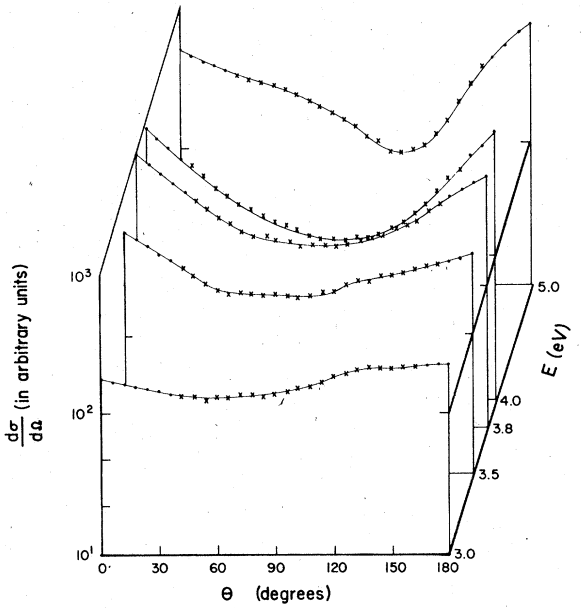

FIG. 4. Three-dimensional perspective plots of angular distribution $d\sigma/d\Omega$ of CO_2 at 3.0, 3.5, 3.8, 4.0, and 5.0 eV impact energies. Dots are extrapolated points.

TABLE I. Angular distribution $d\sigma/d\Omega$ (in normalized counts/sec). (The numbers in parentheses represent extrapolated data points.)

θ° \ E (eV)	3.0	3.5	3.8	4.0	5.0	7.0	10.0	15.0	20.0	30.0	40.0	50.0	70.0	90.0
0														
6	(148)	(432)	(670)	(686)	(389)	(278)	(1094)	(2756)	(6327)	(6834)	(9560)	(7400)	(6545)	(8482)
12	(144)	(386)	(580)	(595)	(356)	(269)	(855)	(1955)	4401	4160	4945	3682	3109	2677
18	(143)	(345)	(510)	(503)	(333)	(259)	(684)	1410	2726	2600	2500	1844	1530	972
24	(143)	(313)	(444)	(435)	(317)	(248)	547	1026	1734	1560	1185	849	649	375
30	(141)	279	384	378	294	234	408	705	1109	847	529	462	306	165
36	(141)	254	334	301	274	223	335	500	751	520	313	255	170	91
42	140	212	289	262	259	208	276	352	494	312	191	144	105	54
48	135	194	260	233	242	198	221	260	336	208	119	90	65	34
54	125	183	233	212	231	194	174	193	237	146	84	60	41	24
60	133	183	217	196	210	181	147	144	184	104	64	46	30	19
66	133	186	217	177	192	164	122	112	127	79	49	35	26	18
72	142	180	206	168	173	148	106	89	98	61	35	31	23	14
78	139	179	197	158	154	136	96	174	82	52	32	27	19	12
84	138	177	188	146	140	123	90	67	65	46	29	24	17	11
90	144	175	185	140	123	116	86	62	64	49	27	20	15	11
96	147	181	188	134	109	103	80	59	67	56	29	20	15	13
102	159	184	187	135	98	96	79	63	73	65	31	21	20	13
108	162	196	196	133	81	92	86	75	91	76	37	32	23	16
114	176	212	208	143	82	93	101	90	109	88	52	46	35	20
120	187	227	214	148	87	98	127	144	126	101	738	67	44	25
126	196	230	224	162	93	108	148	147	160	119	107	97	55	29
132	210	245	240	179	112	128	194	185	199	152	145	132	68	36
138	212	247	252	201	139	157	242	243	244	193	216	171	88	41
144	213	261	280	237	187	196	302	298	309	267	249	212	106	51
150	215	278	334	294	254	251	362	358	373	297	314	255	127	65
156	220	292	377	361	329	310	408	437	414	357	370	297	150	76
162	220	297	423	408	(389)	(363)	(501)	(500)	(527)	(438)	(431)	(339)	(175)	(88)
168	(226)	(317)	(477)	(526)	(467)	(414)	(593)	(583)	(645)	(535)	(486)	(375)	(207)	(102)
174	(228)	(331)	(534)	(625)	(589)	(476)	(718)	(659)	(782)	(669)	(542)	(412)	(240)	(114)

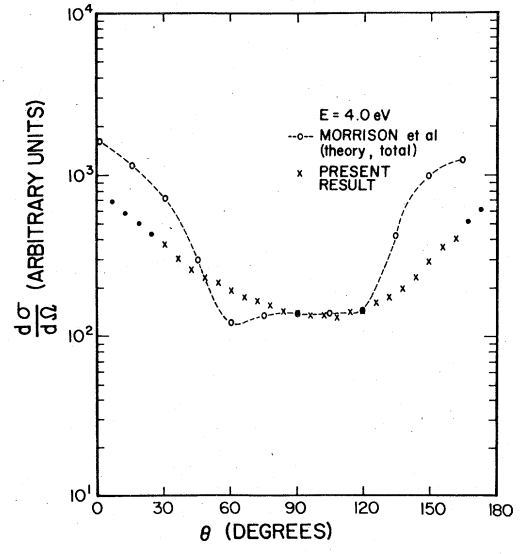

FIG. 5. Angular distribution $d\sigma/d\Omega$ of CO_2 at 4.0-eV impact energy. Comparison with the theoretical calculation of Morrison *et al.* (Ref. 9). Dots are extrapolated points.

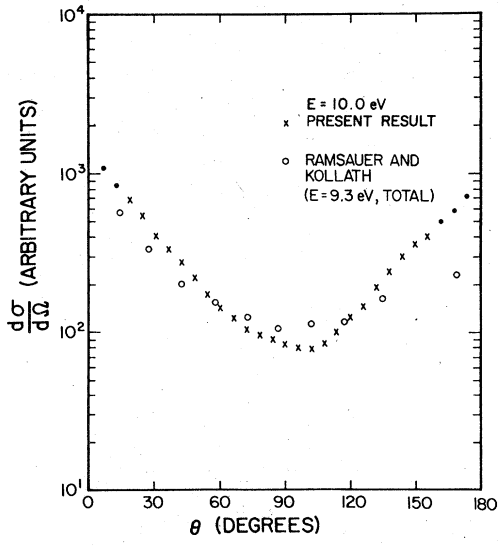

FIG. 6. Angular distribution $d\sigma/d\Omega$ of CO_2 at 10.0-eV impact energy. Dots are extrapolated points. Comparison of Ramsauer and Kollath's measurement at 9.3 eV (Ref. 2).

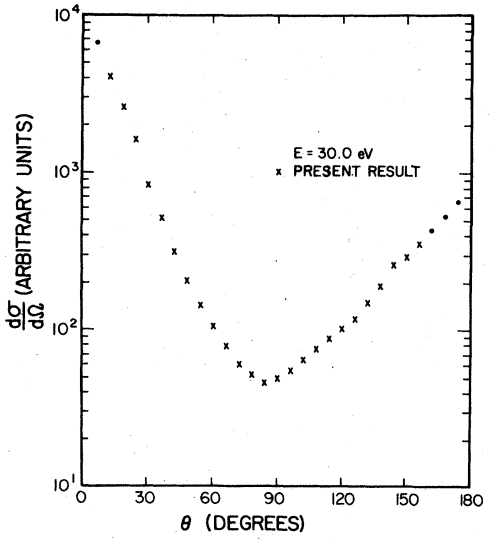

FIG. 7. Angular distribution $d\sigma/d\Omega$ of CO_2 at 30.0-eV impact energy. Dots are extrapolated points.

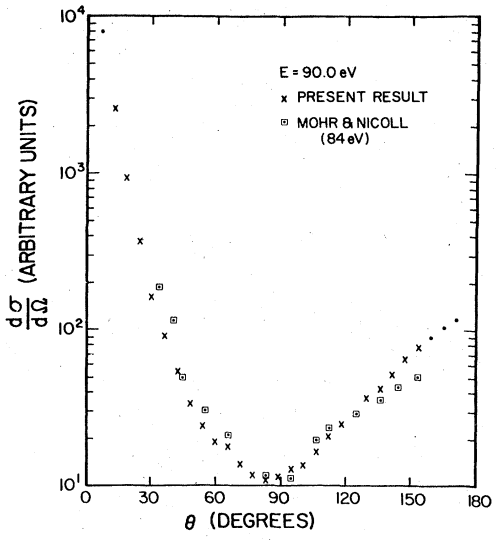

FIG. 9. Angular distribution $d\sigma/d\Omega$ of CO_2 90.0-eV impact energy. Comparison with Mohr and Nicoll's measurement at 84 eV (Ref. 3). Dots are extrapolated points.

state), the distributions show neither a pure S-wave nor P-wave scattering whereas Boness and Schultz[6] assumed isotropic scattering and Danner,[16] who measured the angular distribution at 3.6 eV, found that the scattering was not purely of an S-wave nature.

Figure 5 shows the angular distribution at an incident energy of 4.0 eV along with the theoretical value of the total cross section of Morrison *et al.*[9] For comparison, the theoretical value was normalized to the present data at 90°. The general shapes of the two results are in reasonable agreement, but there is stronger scattering in the forward and backward directions in the theoretical calculations than in the present result. It should be noted that Morrison *et al.*[9] calculated the total scattering cross sections by a fixed-nuclei model which includes elastic and rotationally inelastic scattering cross sections, but not the vibrational cross sections.

The angular distribution at 10.0 eV is shown in Fig. 6 along with the measurement of Ramsauer and Kollath[2] at 9.3 eV. For comparison, the measurement of Ramsauer and Kollath[2] has been normalized at 60° to the present result. The forward scatterings are in fairly good agreement but the backward scattering is lower than that of the present result. The same trend of the angular distributions has been seen at the other energies (3.6 and 6.3 eV) except the strong forward scattering within 15° which may be due to the inelastic scattering cross sections.

Figures 7 and 8 show the angular distributions at 30.0 and 50.0 eV. They have a minimum near 90° and very strong forward and backward scattering.

Figure 9 shows the angular distribution at 90.0 eV and the measurement of Mohr and Nicoll[3] at 84 eV. For comparison, the measurement of Mohr and Nicoll[3] has been normalized at 90° to the present result. The agreement is fairly good except that the ratio of the backscattered component to the forward scattered one is lower than in the present result.

The angular distributions (3.0–90.0 eV) show

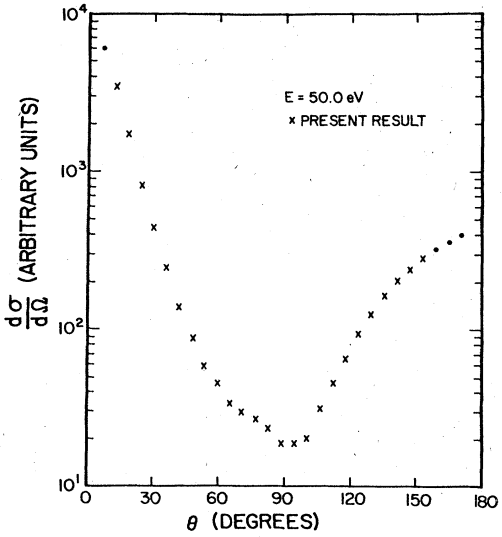

FIG. 8. Angular distribution $d\sigma/d\Omega$ of CO_2 at 50.0-eV impact energy. Dots are extrapolated points.

nearly exponential behavior in the forward and the backward scattering component and these behaviors permit a simple exponential extrapolation to the unmeasured regions of the extreme forward and backward scattering which are required to calculate the total elastic and momentum-transfer cross sections. Since the extrapolation to 0° is over 10° with a steep angular dependence for the higher-energy data (above 20.0 eV), over a wider angular range with a less-steep dependence for the lower-energy data, and the combination of the $\sin\theta$ factor in the calculation of the total elastic cross section, a small uncertainty is expected. The same is true for large-angle side even though the extrapolation is over 20°, since the signal is not changing nearly as rapidly as near 0°.

The total elastic scattering cross sections $\sigma_e(E)$ as a function of energy is given by

$$\sigma_e(E) = \int_0^{2\pi} \int_0^{\pi} \frac{d\sigma}{d\Omega}\, d\Omega\,, \tag{1}$$

where $d\sigma/d\Omega$ is a differential cross section per unit solid angle. The derived cross sections, including the standard deviation, are tabulated in Table II and illustrated in Fig. 10. The energy resolution of 0.06 eV assures discrimination against all three fundamental vibrational modes (oon, ono, and noo), but the rotational excitations are not resolved.

These results are compared to the total cross sections of Brüche and to the calculated total cross sections of Morrison *et al.*[9] The agreement with Brüche's measurement is good from 3.0 to 15.0 eV and at 50.0 eV, but the present result shows a higher value for the elastic cross section between 20.0 and 40.0 eV with a maximum near 20.0 eV. It is noticed that near the 3.8 eV-resonance scattering peak, the width of the shape

TABLE II. Total elastic cross section $\sigma_e(E)$ and momentum-transfer cross section $\sigma_m(E)$ (in units of πa_0^2).

E (eV)	$\sigma_e(E)$	$\sigma_m(E)$
3.0	12.3 ± 1.8	13.5 ± 1.9
3.5	16.7 ± 2.9	16.9 ± 2.9
3.8	19.5 ± 3.0	18.7 ± 2.9
4.0	16.5 ± 3.4	15.4 ± 2.7
5.0	13.9 ± 1.7	12.6 ± 1.6
7.0	12.6 ± 2.2	12.2 ± 2.1
10.0	15.9 ± 2.5	14.7 ± 2.4
15.0	19.8 ± 3.2	14.4 ± 2.3
20.0	27.5 ± 4.4	15.0 ± 2.4
30.0	25.1 ± 3.6	12.9 ± 1.9
40.0	23.2 ± 3.5	10.6 ± 1.6
50.0	17.6 ± 3.2	9.0 ± 1.6
70.0	14.1 ± 2.8	5.4 ± 1.1
90.0	10.7 ± 1.8	2.7 ± 0.5

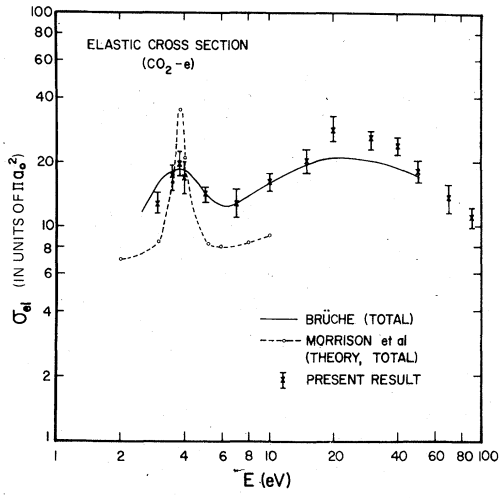

FIG. 10. Elastic scattering cross section in units of πa_0^2. Comparison of the total cross sections of Brüche and the theoretical value of the total cross section of Morrison *et al.* (Ref. 9) with the present result.

resonance is narrower than that of Brüche's as would be expected with the higher resolution.

The agreement with the recent theoretical calculation of Morrison *et al.*[9] is not good below 3.5 and above 5.0 eV. At the 3.8-eV resonance, the total scattering cross section may be in good agreement (within 20%) when the inelastic scattering cross section measured by Spence *et al.*[6] 8.3×10^{-16} cm^2 is added to the elastic peak (the measurement of Spence *et al.*[6] for the inelastic cross section used the trapped-electron method depends on the angular distribution of elastic scattering cross sections).

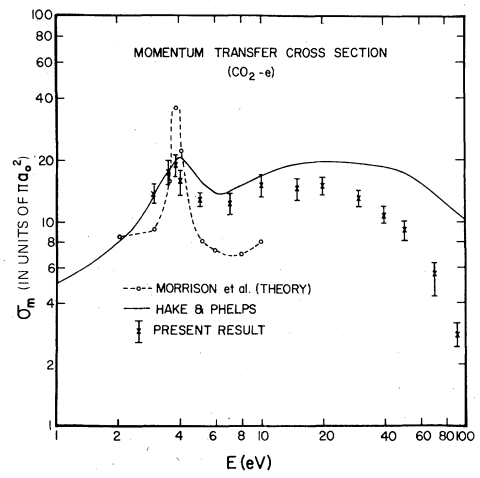

FIG. 11. Momentum-transfer cross section in units of πa_0^2. Comparison of the momentum-transfer cross section of Hake and Phelps (Ref. 8) and the theoretical value of Morrison *et al.* (Ref. 9) with the present result.

The momentum-transfer cross section σ_m which is defined by

$$\sigma_m(E) = \int_0^{2\pi} \int_0^{\pi} \frac{d\sigma}{d\Omega} (1 - \cos\theta)\, d\Omega \qquad (2)$$

can also be derived from the present angular distributions. The result including the standard deviation is given in Table II, and Fig. 11 shows the momentum-transfer cross section calculated from the present results along with those of Hake and Phelps,[8] which are derived from transport coefficients in a swarm experiment, and the theoretical values of Morrison *et al.*[9]

Agreement with the result of the swarm experiment is very good in the low-energy region (<3.8 eV), with an increasing discrepancy with increasing energy. The comparison with Morrison *et al.*[9] reflects the differences observed in the elastic cross sections.

IV. SUMMARY

This paper presents the angular distribution of electrons elastically scattered from CO_2 in the incident energy range 3.0–90.0 eV with angular range −105° to +156°. The elastic cross sections have been normalized among themselves (14 incident energies) and an absolute cross section of CO_2 has been established. The angular distributions were also used to determine the momentum-transfer cross section. The total uncertainty of the elastic cross section and the momentum-transfer cross section is believed to be less than ±15% in standard deviation.

ACKNOWLEDGMENTS

We wish to thank J. Horvath for a useful discussion about the gas inlet system of the apparatus. This work was supported by the Atmospheric Research Section of the National Science Foundation under Grant No. ATM-7617027.

[1]E. Brüche, Ann. Phys. (Leipz.) 83, 1065 (1927).
[2]C. Ramsauer and R. Kollath, Ann. Phys. (Leipz.) 12, 529 (1932).
[3]C. B. O. Mohr and F. H. Nicoll, Proc. R. Soc. A 138, 469 (1932).
[4]E. N. Lassettre, Canadian J. Chem. 47, 1733 (1969).
[5]J. Geiger and K. Wittmaack, Z. Phys. 187, 433 (1965).
[6]M. J. W. Boness and G. J. Schulz, Phys. Rev. Lett. 21, 1031 (1968); D. Spence, J. L. Mauer, and G. J. Schulz, J. Chem. Phys. 51, 5516 (1972).
[7]A. Andrick, D. Danner, and H. Ehrhardt, Phys. Lett. 29A, 346 (1969).
[8]R. D. Hake, Jr., and A. V. Phelps, Phys. Rev. 158, 70 (1967).
[9]M. A. Morrison, N. F. Lane, and L. A. Collins, Phys. Rev. A 15, 2186 (1977).
[10]S. Kumar and D. M. Hunten, J. Geophys. Res. 79, 2529 (1974); D. M. Hunten, G. G. McGill, and A. F. Nagy, Space Sci. Rev. 20, 265 (1977).
[11]D. C. Tyte, Adv. Quantum Electron. 1, 129 (1970).
[12]T. W. Shyn, R. S. Stolarski, and G. R. Carignan, Phys. Rev. A 6, 1002 (1972).
[13]R. W. LaBahn and J. Callaway, Phys. Rev. A 2, 366 (1970).
[14]J. R. Gibson and K. T. Dolder, J. Phys. B 2, 1180 (1969).
[15]J. W. McConkey and J. A. Preston, J. Phys. B 8, 63 (1975).
[16]D. Danner, Ph.D. thesis (Universität Freiburg, 1970) (unpublished).